FROM THE COVER

MOLECULAR ECOLOGY WILEY

Using ultraconserved elements to track the influence of sea-level change on leafy seadragon populations

Josefin Stiller[1,2] | Rute R. da Fonseca[3] | Michael E. Alfaro[4] | Brant C. Faircloth[5] | Nerida G. Wilson[1,6] | Greg W. Rouse[1]

[1]Scripps Institution of Oceanography, University of California San Diego, San Diego, CA, USA

[2]Centre for Biodiversity Genomics, Section for Ecology and Evolution, University of Copenhagen, Kobenhavn, Denmark

[3]The Globe Institute, University of Copenhagen, Kobenhavn, Denmark

[4]University of California Los Angeles, Los Angeles, CA, USA

[5]Department of Biological Sciences and Museum of Natural Science, Louisiana State University, Baton Rouge, LA, USA

[6]Collections & Research, Western Australian Museum, Welshpool and School of Biological Sciences, University of Western Australia, Crawley, WA, Australia

Correspondence
Josefin Stiller, Centre for Biodiversity Genomics, Section for Ecology and Evolution, University of Copenhagen, Kobenhavn, Denmark.
Email: josefin.stiller@bio.ku.dk

Greg W. Rouse, Scripps Institution of Oceanography, University of California San Diego, San Diego, CA, USA.
Email: grouse@ucsd.edu

Funding information
National Geographic Society

Abstract

During the Last Glacial Maximum (LGM), global sea levels were 120–130 m lower than today, resulting in the emergence of most continental shelves and extirpation of subtidal organisms from these areas. During the interglacial periods, rapid inundation of shelf regions created a dynamic environment for coastal organisms, such as the charismatic leafy seadragon (*Phycodurus eques*, Syngnathidae), a brooder with low dispersal ability inhabiting kelp beds in temperate Australia. Reconstructions of the palaeoshoreline revealed that the increase of shallow areas since the LGM was not uniform across the species' range and we investigated the effects of these asymmetries on genetic diversity and structuring. Using targeted capture of 857 variable ultraconserved elements (UCEs, 2,845 single nucleotide polymorphisms) in 68 individuals, we found that the regionally different shelf topographies were paralleled by contrasting population genetic patterns. In the west, populations may not have persisted through sea-level lows because shallow seabed was very limited. Shallow genetic structure, weak expansion signals and a westward cline in genetic diversity indicate a postglacial recolonization of the western part of the range from a more eastern location following sea-level rise. In the east, shallow seabed persisted during the LGM and increased considerably after the flooding of large bays, which resulted in strong demographic expansions, deeper genetic structure and higher genetic diversity. This study suggests that postglacial flooding with rising sea levels produced locally variable signatures in colonizing populations.

KEYWORDS
genetic structure, phylogeography, sea-level changes, Syngnathidae, ultraconserved elements

1 | INTRODUCTION

The shallow parts of the ocean constitute only 9% of the ocean surface (Harris et al., 2014) but harbour a disproportionately rich biodiversity (Costello & Chaudhary, 2017). Much of the continental shelf, the belt of shallow (100–200 m depth) and gradually sloping seabed that surrounds continents, has only become marine habitat since the last ice age (Hewitt, 2000; Provan & Bennett, 2008). Just 21,000–19,000 years ago during the Last Glacial Maximum (LGM), sea levels were 120–130 m lower than today (Lambeck & Chappell, 2001; Yokoyama et al., 2000). The lowered shore was moved to the outer continental shelf or onto the steep continental slope, which reduced shallow habitat by up to 92% (Ludt & Rocha, 2015) and often restricted coastal populations to small and isolated refugia (Bowen et al., 2016; Dolby et al., 2016; Maggs et al., 2008). After the LGM, sea level rose rapidly (Hanebuth et al., 2000) and populations expanded out of refugia and mixed on the newly inundated shelf (Crandall et al., 2012; Dolby et al., 2016, 2018; Jenkins et al., 2018).

Continental shelf populations have therefore experienced significant changes to their environment since the LGM.

Shallow shelf areas did not increase consistently after the LGM but trajectories of increase differed between coasts (Dolby et al., 2020; Holland, 2012). The topography of the continental shelf played a particular role here. Narrow shelves sustained only small habitable areas, at both sea-level lows and highs, while wide margins often experienced strong gains in shallow areas after the LGM (Dolby et al., 2018, 2020). The finding that narrow shelves have a higher diversity of fish species than wide margins (Dolby et al., 2020) implies that different evolutionary forces impacted populations depending on the topography of the coastal segment they inhabit.

When investigating the potential impacts of sea-level change and shelf topography on marine communities, other structuring factors have to be considered. Water temperature is one of the main factors impacting organismal distributions (Bowen et al., 2016) and temperature gradients are often steep along north–south-facing coasts. Temperature may be less significantly structuring the southern Australian coast, the world's longest east–west-facing coastline spanning ~35° of longitude. Particularly, the western and central regions of the south coast have similar mean sea surface temperatures of 16–18°C (http://www.bom.gov.au/cgi-bin/climate/change/averagemaps.cgi?map=sst&season=0112), which are fed by the west-to-east flowing Leeuwin Current. Given this relative temperature stability, putative signatures caused by sea-level change in different coastal segments could be detected more easily than in other parts of the world.

The continental shelves of the western and central regions of Australia's south coast differ in their topography, which impacts the amount of available shallow seabed today and the magnitude of environmental change since the LGM (Figure 1). The central region encompasses South Australia's three large shallow bays: Spencer Gulf (20,000 km^2), Gulf St Vincent (6,800 km^2) and Lacepede Shelf (30,000 km^2) (Murray-Wallace, 2014). These bays were dry during the LGM and the shoreline was up to 450 km offshore (Roberts et al., 2020; Williams et al., 2018). West of the central bays lies the Great Australian Bight (GAB), also with a broad continental shelf. These wide shelves differ from the narrow continental shelf of the western part of the south coast, which descends quickly onto the steep continental slope (Heap & Harris, 2008). In the western areas, the coastline moved only a few kilometers inland when sea level rose (Williams et al., 2018). These different trajectories of postglacial flooding on the wide central and the narrow western shelves may have impacted connectivity and demography of the many species inhabiting these shallow areas. The temperate Australian coast supports an extensive shallow-water system of kelp beds, the Great Southern Reef (Bennett et al., 2016), with an unusually rich seaweed community (Bolton, 1994; Kerswell, 2006) and high endemicity of the associated species (Shepherd & Edgar, 2013). These species probably traced their preferred shallow sunlit bottoms when sea levels rose after the LGM and experienced different postglacial histories depending on their location on the coast. On the narrow western margin, populations are expected to be more differentiated

due to greater patchiness of habitat (Dolby et al., 2020) than on wide margins such as the central bays. On the other hand, because the extent of habitat remained relatively stable on narrow shelves (Dolby et al., 2020), demographic changes may be less pronounced compared to populations on wide margins, which have gained large amounts of habitat.

Here, we investigate population structuring and demographic changes in an iconic endemic fish in relation to regional changes in shallow seabed availability since the LGM. Leafy seadragons—*Phycodurus eques* (Günther, 1865), Syngnathidae—are adapted to hide and hunt in shallow-water kelp with camouflaging dermal outgrowths (Kuiter, 2000). Leafy seadragons range from Cape Leeuwin in the southwestern region of the Great Southern Reef, over the largely inaccessible GAB, to Goolwa in South Australia (https://www.inaturalist.org/taxa/49105-Phycodurus-eques), although the distribution may have been historically wider (Figure 2a) (Baker, 2002, 2005, 2009). Because leafy seadragons are brooders, are slow swimmers and have high site fidelity (Connolly et al., 2002; Connolly et al., 2002), signals of isolation and expansion can be expected to persist for longer in their genomes than in dispersive species in which historical signatures are more readily homogenized by gene flow and introgression (Epps & Keyghobadi, 2015). Consistent with the presumed low dispersal of leafy seadragons, a previous study using microsatellites and mitochondrial DNA found strong differentiation across the range (Stiller et al., 2017). That study also found evidence of demographic expansion in the central bays, which is in line with the postglacial recolonization of these bays, but the relatively low resolution of the seven microsatellites prevented more fine-scale investigations in this part of the coast (Stiller et al., 2017). In the western part of the range, population genetic patterns are largely unknown because previous sampling included only a few individuals.

In this study, we extended sampling and collected genomic data using targeted enrichment of ultraconserved elements (UCEs; Faircloth et al., 2012, 2013; Smith et al., 2014). To understand the geological setting in which leafy seadragon populations occur, we first characterize the shelf topography in the central and western part of the Great Southern Reef and reconstruct the increase in shallow seabed since the LGM. We find that the local differences in shelf topography are paralleled by opposite patterns of genetic diversity and population structuring, suggesting that sea-level change may have produced different population genetic responses in the western and central parts of the coast.

2 | MATERIALS AND METHODS

### 2.1 | Current bathymetry and palaeobathymetry

To compare the distribution of shallow seabed available today and during the LGM across the leafy seadragon's range, we used functions of the R package MARMAP (Pante & Simon-Bouhet, 2013). We used the function getBathy to obtain a contemporary bathymetric
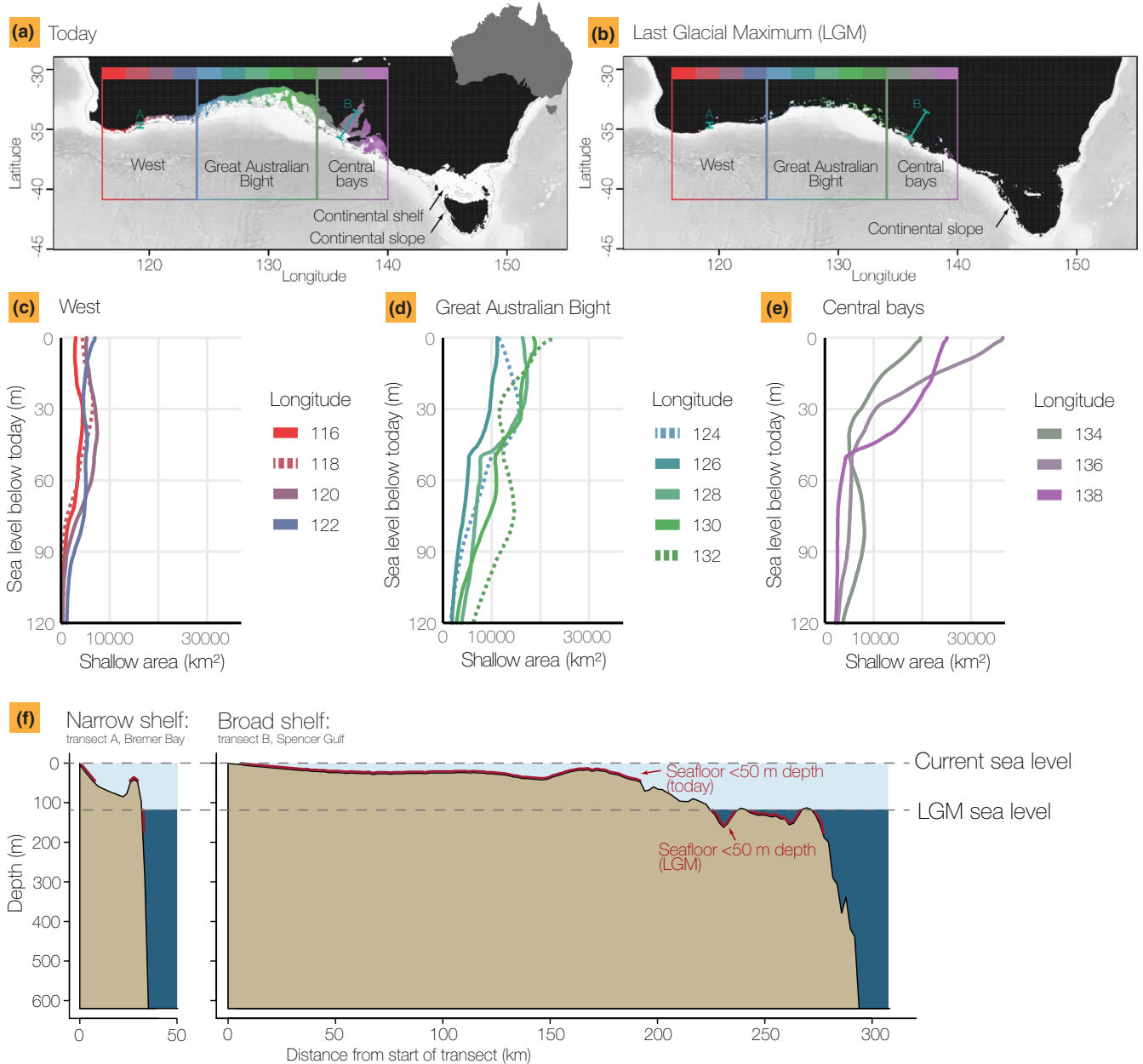
FIGURE 1 Comparison of the southern Australian coast today and during the Last Glacial Maximum (LGM, ~21,000–19,000 years ago). (a) The current shoreline of southern Australia. Within the range of leafy seadragons (*P. eques*), areas of the seafloor that are <50 m deep are highlighted in colours for each 2° longitude. (b) Reconstruction of the shore at the LGM when sea levels were 120 m lower. Subdivision of the coast as in (a). Much of the continental shelf was exposed, reducing the amount of shallow areas. (c–e) Area of available shallow water with varying sea levels from today (0 m) to the LGM (–120 m). Colouring as in (a) for each 2° longitude in: (c) the western part of the south coast, (d) the Great Australian Bight (GAB) and (e) the large bays of the central coast. (f) Cross-section through an area of narrow continental shelf in the western part (transect A) and through an area of a wide continental shelf in one of the central bays (transect B). The locations of the transects are indicated in (a) and (b). Transects are drawn from the shore to the continental slope, with current sea levels in light blue and LGM sea levels in dark blue. The transects have the same scale, showing the greater extent of shallow areas in the central bays

map at a 1-min resolution from the ETOPO1 database on the NOAA server (Amante & Eakins, 2009). The area of shallow seabed that lies between 0 and –50 m in the study region (116–140°W, Figure 2a) was calculated with the getArea function. The lower depth bound was motivated by the local maximum depth of the habitat-forming kelp *Ecklonia radiata* (Marzinelli et al., 2015). Leafy seadragons often

inhabit this kelp but usually at shallower depths (<40 m; Baker, 2009; Kuiter, 2000), making –50 m a conservative depth boundary. The area estimate is not an attempt to quantify seadragon habitat, for which we are missing sufficient information on the distribution of habitat-forming vegetation, wave exposure and sediment type. The estimate for the shallow areas during the LGM was obtained by

(a)

(b) PCA

(c) DAPC K=4

(d) DAPC K=5

(e)
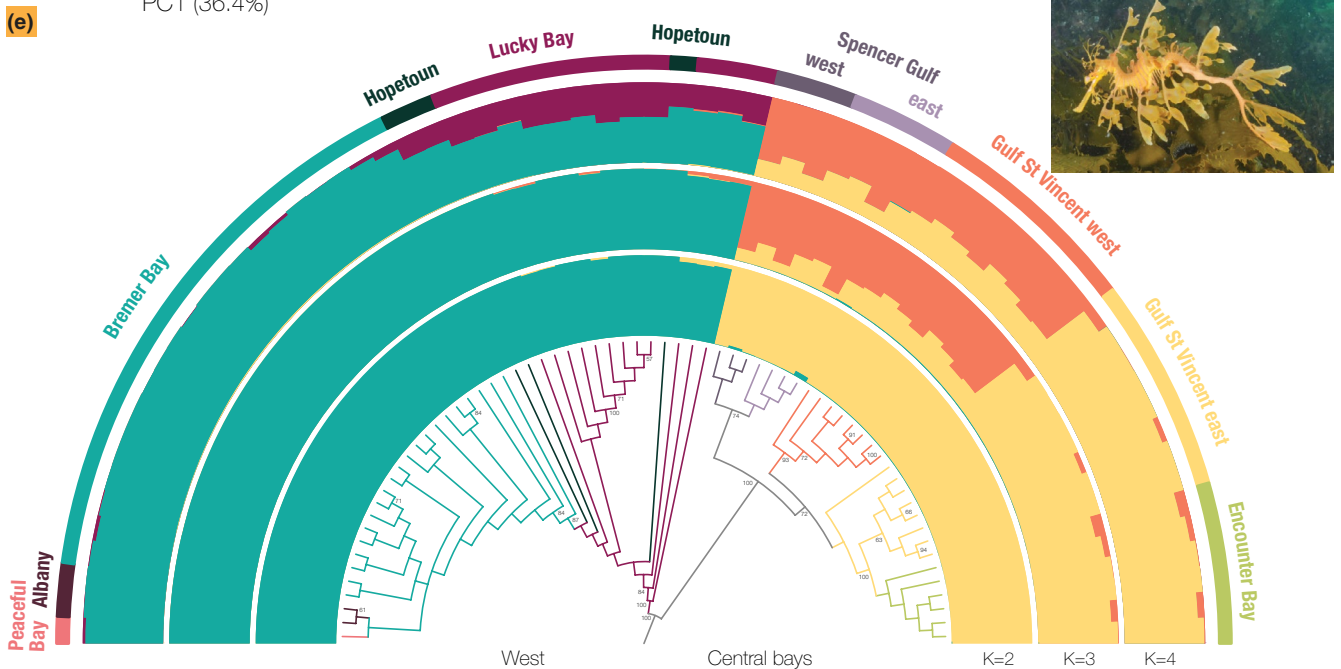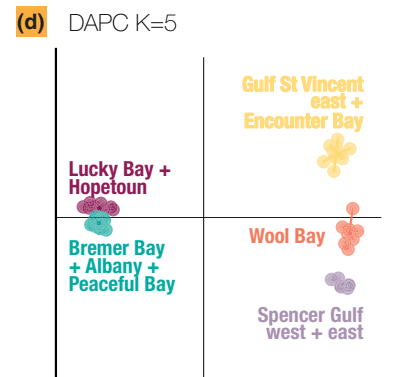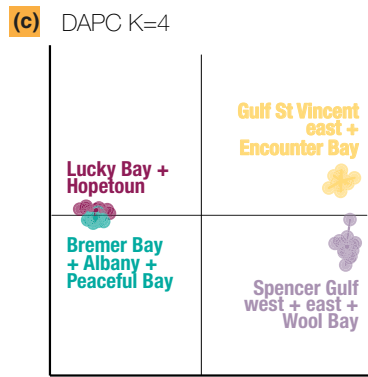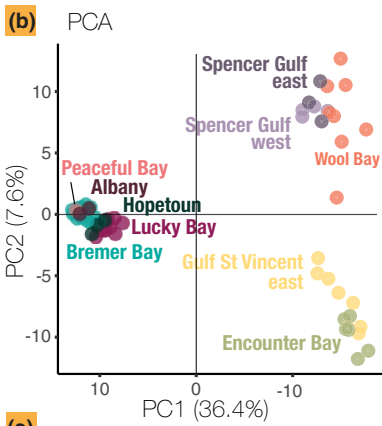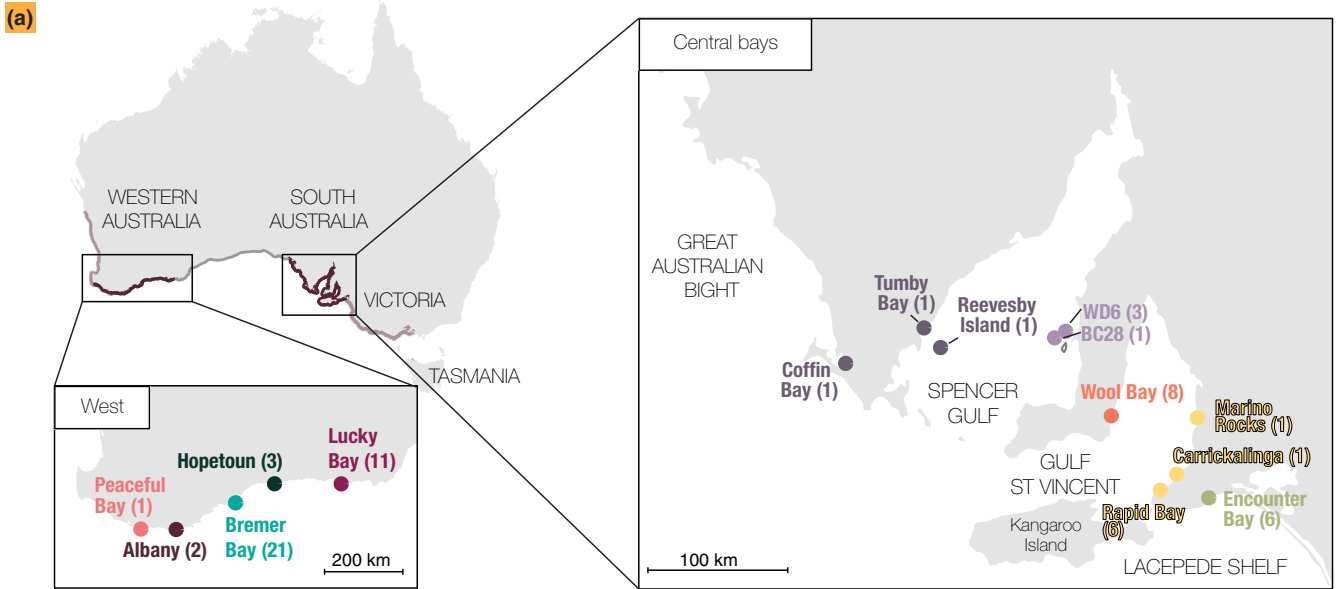
FIGURE 2 Sampling and population structure of leafy seadragons (*P. eques*). (a) Map of Australia showing the species' range in purple, lighter coloured areas representing the range based on historical records. Insets show sampling localities and sample sizes in the western part of the range in Western Australia and the central bays in South Australia. Between the western and eastern sample sites lies a largely inaccessible coast. The dotted line across Yorke Peninsula indicates the location of a marine strait at Peesey Swamp that opened during sea-level highstands. (b) Principal component analysis (PCA) based on the 100% complete data set (224 SNPs) showing the first two PCs. Individuals are represented as dots, coloured by geographical origin but locality information was not used in the analysis. (c, d) Discriminant analysis of principal components (DAPC) based on the 100% complete data set (224 SNPs) for (c) *K* = 4 and (d) *K* = 5 clusters. Individuals are represented by dots, colored by membership to inferred clusters. (e) Individual genetic assignment as inferred by STRUCTURE for *K* = 2 to *K* = 4 and lineage tree from SVDQUARTETS, based on 2,845 SNPs. In the tree, only nodes with >50% bootstrap support are annotated. In the STRUCTURE plots, individuals are represented by bars, which are partitioned into *K* coloured segments showing individual ancestry coefficients. The outermost ring annotates sampling localities. The tree and STRUCTURE admixture proportions were plotted using Anvi'o (Eren et al., 2015)

lowering the sea level to −120 m (Lewis et al., 2013) and calculating bottom area over 50 m depth from the adjusted sea level (i.e., −120 to −170 m below today). To reconstruct the trajectory of area increase with sea-level rise for different coastal segments, we divided the study region into blocks of 2° of longitude (~180 km, Figure 1a,b). In each block, we increased sea level from −120 to 0 m in increments of 1 m and calculated the shallow bottom area over 50 m depth from the adjusted sea level. Using vertical increments of 10 m gave similar trajectories (Figure S1). To gain estimates of contemporary and LGM shallow bottom area specifically around sampling sites, we performed the same calculations for blocks of 2° of longitude centred around sampling sites (Figure S2). To visualize the different shelf topography of the western part and the central bays, transects from representative sampling sites (Bremer Bay, Spencer Gulf) were drawn from shore out to −600 m on the continental slope using MARMAP's get.transect and plotProfile functions.

2.2 | Sampling and permits

Tissue samples from 68 leafy seadragons were sourced from wild or museum specimens (Figure 2a; Table S1). Sampling included 39 of 71 individuals previously sequenced for mitochondrial DNA and microsatellites (Stiller et al., 2017), which had DNA concentrations suitable for library preparation. Ethics approval and collection permits for those tissue samples are given in Stiller et al., (2017). Newly obtained samples came from a total of 29 individuals. New tissue clips were collected from 21 individuals in Western Australia under exemption from the Fish Resources Management Act 1994, Exemption Number 2,726, Department of Fisheries, Western Australia. One sample was obtained from a mortality at the Aquarium of the Pacific, Long Beach, which was the offspring of a brooding male wild-caught in Hellfire Bay, Western Australia. Additional tissues were sourced from the Western Australian Museum, Perth (*N* = 5) and the South Australian Museum, Adelaide (*N* = 2).

We refer to a locality as a sampled geographical site, and to a population as a group of individuals that were sampled near the same locality and were distinguishable by differing allele frequencies (F_{ST}). Localities with only a single individual were grouped with adjacent sites after initial analyses and considering previous findings (Stiller et al., 2017). Populations were subsequently defined as Peaceful

Bay/Albany (*N* = 3), Bremer Bay (*N* = 21), Hopetoun (*N* = 3), Cape Le Grand (Lucky Bay, Hellfire Bay, *N* = 12), Spencer Gulf west (Coffin Bay, Tumby Bay, Reevesby Island, *N* = 3), Spencer Gulf east (stations BC28, WD6, *N* = 4), Wool Bay in the western Gulf St Vincent (*N* = 8), Gulf St Vincent east (Marino Rocks, Carrickalinga, Rapid Bay, *N* = 8) and Encounter Bay on the Lacepede Shelf (*N* = 6) (Figure 2a).

2.3 | DNA extraction, library preparation and targeted capture of UCEs

DNA was extracted from dermal or muscle tissue (dried or stored in ethanol) using the DNeasy Blood & Tissue kit (Qiagen). We quantified DNA using a Qubit fluorometer (Life Technologies). DNA was sheared by sonication with a Bioruptor Standard (Diagenode) into fragments of an average size of 400–700 bp. Genomic DNA libraries were prepared using a commercial kit following the manufacturer's instructions (KAPA Biosystems LTP Library Preparation Kit or KAPA Hyper Prep Kit) with an input of 60–1,200 ng DNA. We used an SPRI beads substitute (Rohland & Reich, 2012) for clean-up steps. Each individual was "barcoded" with single (Faircloth & Glenn, 2012) or dual sequence tags (Glenn et al., 2019). Following adapter ligation, we amplified libraries using the manufacturer's recommended thermal profile and 8–16 PCR (polymerase chain reaction) cycles depending on the input concentration. Reactions were cleaned with SPRI beads and reconstituted in 33 μl double-distilled H_2O (ddH$_2$O). Individual libraries were quantified using Qubit, and libraries from eight individually barcoded samples were pooled at equimolar ratios (62.5 ng each) for target enrichment (500 ng total).

To collect orthologous, putatively unlinked, conserved loci across the nuclear genomes of leafy seadragons, we performed target enrichment of 1,314 UCEs (Alfaro et al., 2018; Faircloth et al., 2013). Although some UCEs can be found in coding regions (White & Braun, 2019), the majority are intergenic and noncoding (Faircloth et al., 2012; McCormack et al., 2012), and the design of enrichment baits (Alfaro et al., 2018) attempts to ensure loci are also independent. To enrich UCEs, we used a commercially synthesized RNA target capture array (UCE Acanthomorph 1Kv1, MyBaits, MYcroarray, Inc.) and followed the manufacturer's target enrichment protocol (versions 2 and 3). For hybridization to the synthetic RNA probes, genomic DNA was incubated with blocking agents as supplied

by MYcroarray and with a custom block against the barcodes. Hybridization was performed in a thermocycler for 24 hr at 65°C. For post-hybridization washes, we followed MYcroarray's protocol but included a size selection using 1× SPRI beads to remove small fragments. The enriched DNA was eluted in 30 µl of nuclease-free H_2O and amplified using KAPA HiFi HotStart Ready Mix following the recommended thermal profile and 16–18 PCR cycles. Reactions were cleaned using SPRI beads, reconstituted in 22 µl ddH$_2$O, and quantified using Qubit prior to pooling for sequencing.

Samples were sequenced on the MiSeq (Illumina) platform, using one run with 500 cycle (= 250 bp paired end [PE]) version 2 chemistry and four runs with 600 cycle (= 300 bp PE) version 3 chemistry at the UCSD Stem Cell Genomics Core. We also used two partial lanes of the HiSeq2500 (Illumina) in Rapid Run mode generating 100 bp PE data, and one partial lane of the HiSeq4000 (Illumina) generating 100 bp PE data at the UCSD IGM Genomics Center.

2.4 | Bioinformatic processing

Raw reads were cleaned from adapter contamination and low-quality bases with TRIMMOMATIC version 0.39 (Bolger et al., 2014) using ILLUMIPROCESSOR version 2.0.2 (Faircloth, 2013). We produced a reference assembly of UCE loci and their flanking regions for one individual (WAM P.33854–001) using scripts implemented in PHYLUCE version 1.5 (Faircloth, 2016). We assembled contigs with VELVET version 1.2.10 (Zerbino & Birney, 2008) with k-mers ranging from 25 to 75 in increments of 10. Among these contigs, we selected the longest contig for each UCE locus as the reference. Sequence reads of each sample were mapped against the reference with BWA version 0.7.17 mem (Li & Durbin, 2009) and processed with SAMTOOLS version 1.9 (Li et al., 2009). The following steps were performed with tools implemented in GATK version 4.1.4.0 (DePristo et al., 2011; McKenna et al., 2010). MarkDuplicates was used to filter PCR duplicates, read groups were added with AddOrReplaceReadGroups and BAM files from individuals that were sequenced on multiple sequence runs were combined with MergeSamFiles. Sequencing, mapping and deduplication statistics for runs and samples are given in Tables S2 and S3. Single nucleotide polymorphisms (SNPs) for each sample were called with HaplotypeCaller in GVCF mode. Individual GVCF files were combined with COMBINEGVCFS and genotyped using GenotypeGVCFs. Variants were filtered for quality using VariantFiltration (parameters in Supporting Information) and only biallelic SNPs were retained. VCFTOOLS version 0.1.17 (Danecek et al., 2011) was used to only include genotypes with ≥10× depth of coverage in each individual and with a minor allele frequency of ≥0.05, resulting in 2,845 SNPs. We also created a data set without missing data with 224 SNPs.

2.5 | Assignment of individuals to genetic clusters

To investigate genetic affinities of individuals, we used principal component analysis (PCA) and discriminant analysis of principal components (DAPC) on the data set without missing data. PCA was run with the R package ADE4 (Dray et al., 2007) and plotted using the first two PCs to summarize the overall variability among individuals. DAPC assigns individuals to a predefined number of K groups using all PCs and k-means clustering, maximizing differences between groups while ignoring variation within groups (Jombart et al., 2010). DAPC was performed with the R package ADEGENET (Jombart, 2008) in 100 replicates from $K = 1$ to $K = 8$. We then investigated the clustering solutions with the lowest Bayesian Information Criterion (BIC), keeping the PCs that captured >80% of the cumulative variance.

To quantify admixture proportions of individuals, we used the Bayesian clustering method STRUCTURE version 2.3.4 (Pritchard et al., 2000) using PARALLELSTRUCTURE (Besnier & Glover, 2013) on the CIPRES ScienceGateway (Miller et al., 2010). Using the 2,845 SNPs data set, we tested $K = 1$ to $K = 8$ in five replicates using 500,000 Markov chain Monte Carlo (MCMC) iterations, of which 100,000 were discarded as burnin. Consensus clustering across replicate runs was generated on the CLUMPAK server (Kopelman et al. 2015). Clustering solutions of all tested K were investigated, and we also report the K chosen with the ΔK method (Evanno et al., 2005) and the plateau of the log likelihood (Pritchard et al., 2000) as determined using the STRUCTUREHARVESTER server (Earl & vonHoldt, 2012).

To estimate relationships among leafy seadragon individuals in a coalescent tree-based framework, a tree of all individuals was built with SVDQUARTETS (Chifman & Kubatko, 2014) in PAUP* version 4.0a166 (Swafford, 2002). We used 2,845 SNPs to generate a lineage tree using 200,000 random quartets and 100 bootstrap replicates.

2.6 | Population genetic differentiation and spatial patterns

After delineation of populations through clustering and tree-based analyses, we investigated genetic differentiation using 2,845 SNPs to calculate F_{ST} and F'_{ST} between populations. F'_{ST} is standardized to the maximum possible value given the amount of diversity within the population to allow for better comparability between different markers and organisms (Hedrick, 2005). We assessed statistical significance with 1,000 permutations in GENODIVE version 3.01 (Meirmans, 2020).

To investigate possible isolation by distance (IBD), pairwise F_{ST} between populations was correlated with geographical distances using a Mantel test. Because hierarchical population structure has been previously identified at least in the eastern part of the range (Stiller et al., 2017), we also employed a stratified Mantel test (Meirmans, 2012) permuting populations within the eastern and western clusters. Mantel tests were run in GENODIVE with 1,000 permutations to assess statistical significance. Geographical distances between sites were calculated as least-cost distances. By incorporating the additional distance a coastal organism has to travel around land and around uninhabitable deep water, least-cost distances give a more realistic representation of traversal distances than straight-line distances (Etherington, 2016). Pairwise distances were calculated on

the bathymetric grid with MARMAP's trans.mat and lc.cost functions, while restricting the path to depths between 0 m (avoiding land) and −50 m (avoiding deep waters, while allowing traversal 10 m below the maximum recorded depth of leafy seadragons). For populations with multiple localities, we selected one sampled site to represent the population (Table S4).

Because methods that explicitly incorporate geographical origins of individuals can sometimes discern more subtle population structure (Peter et al., 2019), we used EEMS (Petkova et al., 2016) to visualize the spatial patterns of genetic structure. EEMS finds deviations from IBD and estimates local rates of effective migration and genetic diversity on a geographical grid. The grid was given as a polygon of the range of leafy seadragons outlined to the edge of the continental shelf (drawn with https://www.keene.edu/campus/maps/tool/). The polygon was split into 700 demes, which allowed sampling localities to reside in separate demes. We used 2,845 SNPs in two runs from different starting seeds, 5 million MCMC iterations, 1 million burnin and 9,999 thinning iterations. The runs were checked for convergence and analyzed together with the R package REEMSPLOTS (Petkova et al., 2016).

2.7 | Characterization of genetic diversity

We calculated individual-level heterozygosity across the 2,845 SNPs using VCFTOOLS and divided the number of observed heterozygous sites by the number of genotyped SNPs. We calculated the observed (H_O) and expected heterozygosity (H_E) for each population in GENODIVE. To test whether geographical regions differed significantly in their genetic diversity, we compared H_E and H_O between the western and central bay groups with the OSx test statistic (Goudet, 1995) using 1,000 randomizations of the populations between groups. We tested for correlation of population-level H_O with the increase in area of local shallow seabed since the LGM by fitting a linear model in R.

To investigate signals of expansion, we calculated Tajima's D using the R library PEGAS (Paradis, 2010). The 2,845 SNPs were placed onto the UCE reference assembly using BCFTOOLS version 1.9 (Li, 2011), encoding missing genotypes as N and heterozygous sites as IUPAC ambiguity codes. We calculated Tajima's D for populations with more than three individuals, for all individuals of the eastern and the western clade, and across the entire data set.

2.8 | Tests of phylogeographical scenarios

To determine which historical scenarios were most compatible with observed genetic structuring, we used approximate Bayesian computation in DIYABC version 2.1.0 (Cornuet et al., 2014). We tested simple scenarios separately for the western and the central group with a focus on distinguishing between population splitting scenarios for which we had empirical or theoretical evidence. In the western group, we excluded two populations because of their low sample

size ($N = 3$). For the better sampled Cape Le Grand and Bremer Bay populations, we tested a colonization from east to west (supported by the SVDQUARTETS tree), against colonization from west to east (the direction of the Leeuwin Current), against the same two models but with a reduced effective population size in the newly colonized population (supported by a cline in heterozygosity). In the central bays, we grouped samples from Spencer Gulf ($N = 9$), which had relatively low genetic differentiation and were a clade in the lineage tree. We were specifically interested in inferring the directionality of the colonization of eastern Gulf St Vincent. We tested a stepwise colonization strictly from west to east (supported by the SVDQUARTETS tree), against a scenario where Encounter Bay gave rise to the more western Gulf St Vincent east (the opposite route for this population pair), against a model of instantaneous divergence.

For phylogeographical modeling, we selected one SNP from each of the 857 variable UCE loci that was genotyped across the highest number of samples. According to DIYABC's requirements, we further excluded SNPs that were missing in all individuals of one of the populations or that were monomorphic across the western or eastern cluster, resulting in 258 and 350 SNPs respectively (Table S5). After initial runs, summary statistics that were identified as unfitting by DIYABC's model checking procedure (Cornuet et al., 2010) were removed (Table S5). We used broad uniform priors on effective population sizes (10–500,000; 10–100,000 for bottlenecks) and on event timing, with an upper bound at the LGM (10–19,000 years; Table S6). Little is known about the life history of leafy seadragons; we assumed a generation time of 1 year, borrowing from estimates of the related common seadragon (11–16 months; Sanchez-Camara et al., 2005) and other syngnathids (Braga Goncalves et al., 2017; Curtis & Vincent, 2006). A total of 200,000 data sets were simulated for each scenario. Posterior probabilities of scenarios were calculated by logistic regression on the 1% of the simulations that were closest to the observed values and the posterior distribution of parameters was estimated for the best-supported scenario.

3 | RESULTS

3.1 | Availability of shallow seabed today and during the LGM

At current sea levels, the total area of shallow seabed within the upper 50 m along the southern coast of Australia (116–140°W) was estimated at 179,070 km^2 (Figure 1a). During the LGM, when sea level was at −120 m, there was 85% less area with bottom depths potentially suitable to establish seadragon habitat (26,643 km^2, Figure 1b). The trajectories of flooding of shallow areas since the LGM was uneven in different parts of the southern coast (Figure 1c–e). We discuss neighbouring coastal sections of 2° longitude in three groups based on similar trajectories, namely the west (116–122°W with four sections), GAB (124–132°W with five sections) and central bays (134–138°W with three sections). In the western sections, the trajectory of increase in shallow

seabed since the LGM was relatively flat (Figure 1c). During the LGM, shallow areas were very limited (229–1,154 km^2 in each section, total 2,027 km^2), particularly in the westernmost sections (229–361 km^2) while the area bordering the GAB retained more shallow seabed during the LGM (1,154 km^2). This corresponds to a 90% reduction of shallow areas in the western region during the LGM compared to today (3,010–6,960 km^2 in each section, total 19,626 km^2). In the GAB, gains in shallow seabed followed steeper trajectories (Figure 1d). During the LGM, large shallow stretches remained (1,603–6,204 km^2 in each section, total 16,268 km^2) and the extent of shallow seabed increased consistently until today (11,153–22,037 km^2 in each section, total 79,561 km^2). In the central part of the coast, shallow areas increased steeply after sea level rose past −50 m marking the flooding of the central bays (Figure 1e). Relatively large areas of shallow seabed existed during the LGM (2,251–3,682 km^2, total 8,578 km^2), but this was still 89% less than the shallow areas in existence today in the central bays (19,639–36,539 km^2, total 81,250 km^2).

The relative change in shallow seabed area since the LGM was therefore similar across the coast but the absolute amount of habitat gained was much larger in the central parts and the GAB compared to the western regions. With respect to our leafy seadragon sampling, which does not cover the GAB, there is today about 314% more shallow seabed in the central coast compared to the west. This is despite the fact that the central coast, as delineated here, spans 2° of longitude less than the western coast. The reasons for these regional differences lie in the topography of the coastal segments (Figure 1f). The narrow continental shelf of the western coast quickly tapers onto the continental slope, which limits the current area of shallow seabed. During the LGM, shallow areas were even more restricted because the shore was located on the steep continental slope. This stands in contrast to the central coast, where today's continental shelf is expansive due to its gradual slope. During the LGM, the shore was still located on the continental shelf, albeit with shallow areas being smaller than today (Figure 1f).

3.2 | Population genetic sequencing of UCEs

After quality and adapter trimming, each sample had on average 2,705,473 reads (range 605,596–8,572,702; Table S3). A total of 1,186 UCE loci were assembled for the reference with an average length of 928 bp (range 102–2,421 bp) and a total length of 1,100,217 bp. On average, 48% of reads of each sample mapped to the reference loci (range 23%–73%). After SNP calling and variant filtration, a total of 2,845 SNPs were identified (mean coverage 32×), of which each sample had on average 48% of the SNPs genotyped (range 24%–92%; Table S3). In the data set with one SNP on each of the 857 variable UCEs (mean coverage 44×), each sample had on average 67% of the SNPs genotyped (range 32%–96%).

3.3 | Assignment of leafy seadragon individuals to genetic clusters

PCA grouped the samples into three clusters (Figure 2b). The first two PCs explained 44% of the genetic variation and the remaining PCs accounted for <6% (Figure S3). The first PC separated samples from the western part of the range from samples of the central bays. The second PC separated samples within the central bays into a cluster of Wool Bay + Spencer Gulf and a cluster of Gulf St Vincent east + Encounter Bay. All individuals from localities in the western part of the range clustered tightly and separation of a particular geographical site was not possible.

DAPC indicated $K = 4$ groups (BIC = 208.46) but $K = 5$ produced a similar value (BIC = 208.75; Figure S4). We consider both solutions here. At $K = 4$, two clusters were found in the west, comprising Peaceful Bay/Albany + Bremer Bay and Hopetoun + Cape Le Grand, and two clusters in the central part of the coast, namely Wool Bay + Spencer Gulf and Gulf St Vincent east + Encounter Bay (Figure 2c). At $K = 5$, additional structure emerged in the central bays, with Spencer Gulf and Wool Bay separating into different clusters (Figure 2d).

Individual-based clustering with STRUCTURE supported an optimal number of clusters at $K = 2$ with the ΔK method and at $K = 4$ where the log likelihood plateaued (Figure S5). We show the clustering solutions in that range (Figure 2e, $K = 5$–8 in Figure S6). A single cluster $K = 1$ can be excluded because of a considerably worse log likelihood than for higher values. At $K = 2$, the samples separated between the western and the central coast (Figure 2e). Some individuals of the easternmost population of the western group (Cape Le Grand) and of the westernmost populations of the central coast (Spencer Gulf east and west) showed small proportions of admixture. At $K = 3$, additional substructure was detected among the central bays, splitting into an eastern (Spencer Gulf + Wool Bay) and a western group (Gulf St Vincent east + Encounter Bay). At $K = 4$, further substructure was identified in the western group with an ancestry component added for samples from Cape Le Grand and Hopetoun. Some samples from Bremer Bay and Peaceful Bay/Albany also showed low proportions of this ancestry component.

The lineage tree from SVDQUARTETS was rooted on the split between the western and central coast groups, which was identified as the deepest genetic divergence by PCA, DAPC and STRUCTURE. Bootstrap support of individual relationships from nearby localities was low (<50%), as expected for individuals in genetic exchange, but populations in the central bays were mostly supported as clades with moderate bootstrap support (Figure 2e; branch lengths in Figure S7). In the central bays, individuals from Spencer Gulf formed a clade. Different from the clustering-based analyses, samples from the eastern and western part of Spencer Gulf were separated (bootstrap support = 66). Wool Bay individuals formed a clade as the sister group to samples from further east. Most samples from the eastern Gulf St Vincent formed a clade with the exception of the individual from Carrickalinga (code e033), which

was the sister group to a well-supported clade (bootstrap support = 100) of the remaining eastern Gulf St Vincent east samples and those from Encounter Bay. In contrast to this relatively strong structure in the central bays, most populations from the western coast were not supported as clades, with the Cape Le Grand population containing all other populations from further west, the individuals from Hopetoun interspersed among Cape Le Grand individuals, and the Bremer Bay group including Peaceful Bay and Albany individuals.

3.4 | Spatial genetic structure

Allele frequency differences were high and statistically significant between most populations (Table 1). Differentiation was highest between populations of the western and the central coast (maximum $F_{ST} = 0.588$, $F'_{ST} = 0.702$, $p < .001$). In the western group, the geographically proximate populations of Peaceful Bay/Albany and Bremer Bay showed weak differentiation ($F_{ST} = 0.040$, $F'_{ST} = 0.036$, $p < .01$), as did Hopetoun and Cape Le Grand ($F_{ST} = 0.056$, $p < .01$, $F'_{ST} = 0.051$, $p < .05$). Peaceful Bay/Albany and Hopetoun were moderately differentiated ($F_{ST} = 0.141$, $F'_{ST} = 0.157$) but the comparisons were not significantly different, probably due to the low sample size ($N = 3$ each). In the central bays, samples from the western and the eastern part of Spencer Gulf had low differentiation ($F_{ST} = 0.046$, $p < .05$, $F'_{ST} = 0.054$, not significant). Both populations were significantly differentiated from Wool Bay in the western Gulf St Vincent, with samples from the eastern Spencer Gulf being less differentiated ($F_{ST} = 0.091$, $p < .001$, $F'_{ST} = 0.124$, $p < .01$) than those from the western Spencer Gulf ($F_{ST} = 0.103$, $F'_{ST} = 0.125$, $p < .01$). Wool Bay was strongly differentiated from the neighbouring population

in Gulf St Vincent east ($F_{ST} = 0.192$, $F'_{ST} = 0.255$, $p < .001$) and the easternmost site Encounter Bay ($F_{ST} = 0.166$, $p < .001$, $F'_{ST} = 0.218$, $p < .01$). Gulf St Vincent east and Encounter Bay were moderately but significantly differentiated ($F_{ST} = 0.085$, $F'_{ST} = 0.104$, $p < .001$).
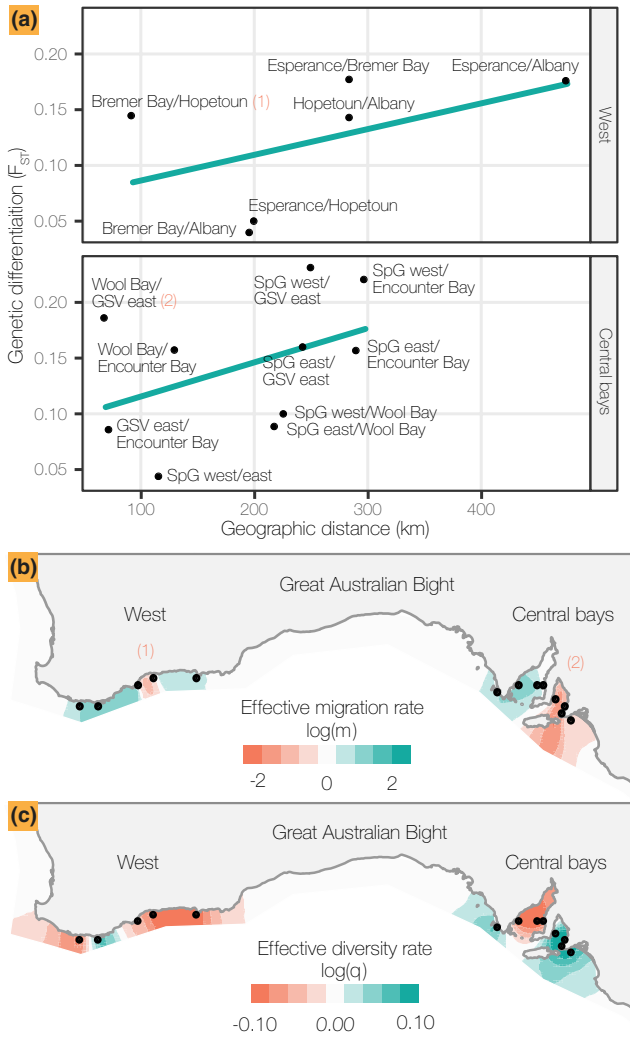
There was a significant correlation between geographical least-cost distances (Figure S8) and F_{ST} using both a standard Mantel test (Mantel's $r = 0.966$, $p < .001$) and a stratified Mantel test (Mantel's $r = 0.966$, $p < .05$). Nonetheless, the spatial patterns differed between the two groups (Figure 3a). Differentiation was weaker in the western part of the range than in the central bays (maximum $F_{ST} = 0.178$ vs. 0.232), even though the sites on the western coast spanned a greater geographical distance than the eastern sites (maximum least-cost distance 476 vs. 298 km). A few populations stood out where differentiation did not strictly follow IBD (Figure 3a). In particular, Wool Bay in the western Gulf St Vincent and sites in the eastern Gulf St Vincent had unexpectedly high differences in allele frequencies ($F_{ST} = 0.192$) despite being only 69 km apart. In fact, their differentiation was on the order of sites that are at least 240 km apart (Figure 3a). In comparison, sites at similar geographical distance (Gulf St Vincent east vs. Encounter Bay, 73 km; eastern vs. western Spencer Gulf, 117 km) were less differentiated ($F_{ST} = 0.085$ and 0.046; Figure 3a) than the sites on opposite legs of Gulf St Vincent.

This deviation from the expectation of IBD was also detected by EEMS, which inferred the lowest effective migration rates between individuals from Wool Bay and Gulf St Vincent east (Figure 3b). In the western part of the coast, effective migration rates were generally higher, with the exception of lowered rates between Hopetoun and Bremer Bay (Figure 3b). Effective diversity rates were also not evenly distributed, being generally lower in the west (except for Albany) than in the central bays (Figure 3c).

TABLE 1 Population differentiation among leafy seadragons (*P. eques*) from 2,845 SNPs; comparisons are pairwise F_{ST} values (above the diagonal) and standardized F'_{ST} (below diagonal) with significance levels indicated by asterisks

F'_{ST}/F_{ST}	Peaceful Bay/Albany	Bremer Bay	Hopetoun	Cape Le Grand	Spencer Gulf west	Spencer Gulf east	Wool Bay	Gulf St Vincent east	Encounter Bay
Peaceful Bay/Albany	—	0.040**	0.141	0.173**	0.568	0.509*	0.492**	0.520**	0.526*
Bremer Bay	0.036**	—	0.148***	0.171***	0.568***	0.469***	0.543***	0.588***	0.577***
Hopetoun	0.157	0.157***	—	0.056**	0.497	0.462*	0.481**	0.502**	0.509**
Cape Le Grand	0.210**	0.192***	0.051*	—	0.491**	0.418**	0.476***	0.526***	0.521***
Spencer Gulf west	0.623	0.641***	0.558	0.554**	—	0.046*	0.103**	0.234*	0.223**
Spencer Gulf east	0.592*	0.571**	0.553*	0.523**	0.054	—	0.091***	0.164**	0.163**
Wool Bay	0.607**	0.658***	0.580**	0.578***	0.125**	0.124**	—	0.192***	0.166***
Gulf St Vincent east	0.632**	0.702***	0.613**	0.636***	0.292**	0.225**	0.255***	—	0.085***
Encounter Bay	0.639*	0.701***	0.613*	0.630***	0.265**	0.218**	0.218**	0.104***	—

Note: Significance levels: *$p < .05$, **$p < .01$, ***$p < .001$.

(a)

(b) West / Great Australian Bight / Central bays

Effective migration rate
log(m)

-2   0   2

(c) West / Great Australian Bight / Central bays

Effective diversity rate
log(q)

-0.10   0.00   0.10

FIGURE 3 Spatial patterns in genetic similarity among leafy seadragons (*P. eques*). (a) Relationship of least-cost distances between sampling localities and genetic differentiation (F_{ST}). Note the greater geographical extent of western sites but their lower differentiation. Numbers denote two population pairs with lower than average effective migration rate inferred by EEMS. Abbreviations: SpG, Spencer Gulf; GSV, Gulf St Vincent. (b, c) Smoothed contour maps showing the average posterior mean of (b) effective migration rates (*m*), which quantify how fast similarity between two individuals decays across geographical space, and (c) effective diversity rates (*q*), which express how dissimilar two individuals from the same location are expected to be. Black dots are sampling sites. Rates are on a log_{10} scale relative to overall mean rates with positive values denoting rates above average and negative values indicating rates below average

3.5 | Genetic diversity

Heterozygosities were significantly lower in the western group than in the central bays both at the individual level (Wilcoxon rank sum test, $p < 2.2e^{-16}$) and the population level (OSx $H_O = 0.095$, $p < .01$, OSx $H_E = 0.083$, $p < .01$; Table 2). In the western cluster, there was

TABLE 2 Genetic diversity of leafy seadragon (*P. eques*) populations across 2,845 SNPs

Population	N	H_O	H_E	Tajima's D
Western group	39	0.178	0.159	−3.746[***]
Peaceful Bay/Albany	3	0.182	0.140	—
Bremer Bay	21	0.167	0.143	−4.108[***]
Hopetoun	3	0.207	0.174	—
Cape Le Grand	12	0.216	0.177	−4.684[***]
Central bays	29	0.275	0.268	−4.111[***]
Spencer Gulf west	3	0.251	0.220	—
Spencer Gulf east	4	0.306	0.224	−9.925[***]
Wool Bay	8	0.290	0.247	−5.382[***]
Gulf St Vincent east	8	0.240	0.213	−5.481[***]
Encounter Bay	6	0.267	0.232	−6.327[***]
Total	68	0.235	0.201	−3.513[***]

Note: Tajima's D could only be calculated for populations with more than three individuals.

Abbreviations: H_E, expected heterozygosity; H_O: observed heterozygosity; *N*, number of samples.

***Significance levels: $p < .001$.
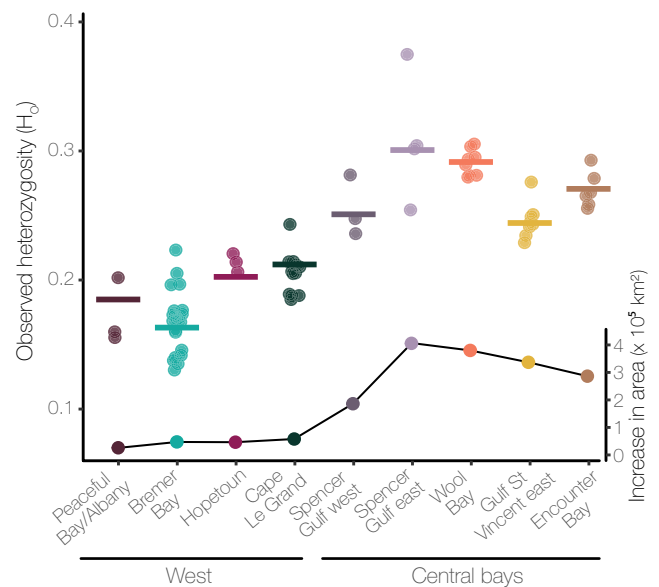
FIGURE 4 The gain of shallow seabed since the LGM correlates with heterozygosity of leafy seadragons (*P. eques*). Dots show individual-level observed heterozygosity (H_O) for 68 individuals and bars indicate population-level H_O. Populations are arranged from west to east. The line graph shows the increase in shallow seabed area (<50 m) since the LGM (Figure S2). For populations with multiple sampling localities, one locality was chosen (Table S4)

a decline in heterozygosity westward, while heterozygosity varied between sites in the central bays (Figure 4). We found that the increase of shallow seabed area since the LGM calculated around sampling localities closely traced the population-level H_O ($R^2 = 0.809$,

p < .001; Figure 4). Tajima's *D* was negative across all populations (Table 2) with stronger signals of expansion in eastern populations (*D* = −5.383 to − 9.925) than in western populations (*D* = −4.108 and − 4.677).

3.6 | Scenario testing

Model testing with DIYABC for the western group supported an east-to-west expansion with a reduced population size in the newly founded Bremer Bay population (Figure 5; Figures S9 and S10). A scenario of colonization following the direction of the Leeuwin Current (west to east) was not supported. The split of Bremer Bay from the ancestor of the Cape Le Grand population was dated to a median of 15,500 years ago (2.5%–97.5% quartile: 6,240–18,800) and the recovery from the bottleneck was dated to a median of 5,400 years ago (2.5%–97.5% quartile: 419–14,100 years ago; Table S7). In the east, the favoured scenario was an eastward splitting but with a west-to-east colonization of eastern Gulf St Vincent from Encounter Bay (Figure 5; Figure S9). This indicates that Gulf St Vincent was colonized twice,

once from the west around 6,930 years ago (median, 2.5%–97.5% quartile: 2,350–13,700 years ago) and a second time from the east (Encounter Bay) around 2,280 years ago (median, 2.5%–97.5% quartile: 296–7,090 years ago; Table S7).

4 | DISCUSSION

4.1 | The change of the shore in temperate Australia since the LGM

This study suggests that regionally different trajectories of increase in shallow shelf area since the LGM caused contrasting responses in populations of a marine fish. Across the leafy seadragon's range, we estimated that the amount of shallow shelf area (0–50 m depth) was 85% smaller during the LGM than today because in many areas the shore fell below the shelf break onto the steep continental slope (Figure 1f). These estimates align with reductions of global estuaries by 82% during the LGM (Dolby et al., 2020), by 75%–92% in shallow tropical regions (calculated over 0–60 m; Ludt & Rocha, 2015) and by 92% in very shallow areas on the Sunda Shelf (0–10 m; Crandall
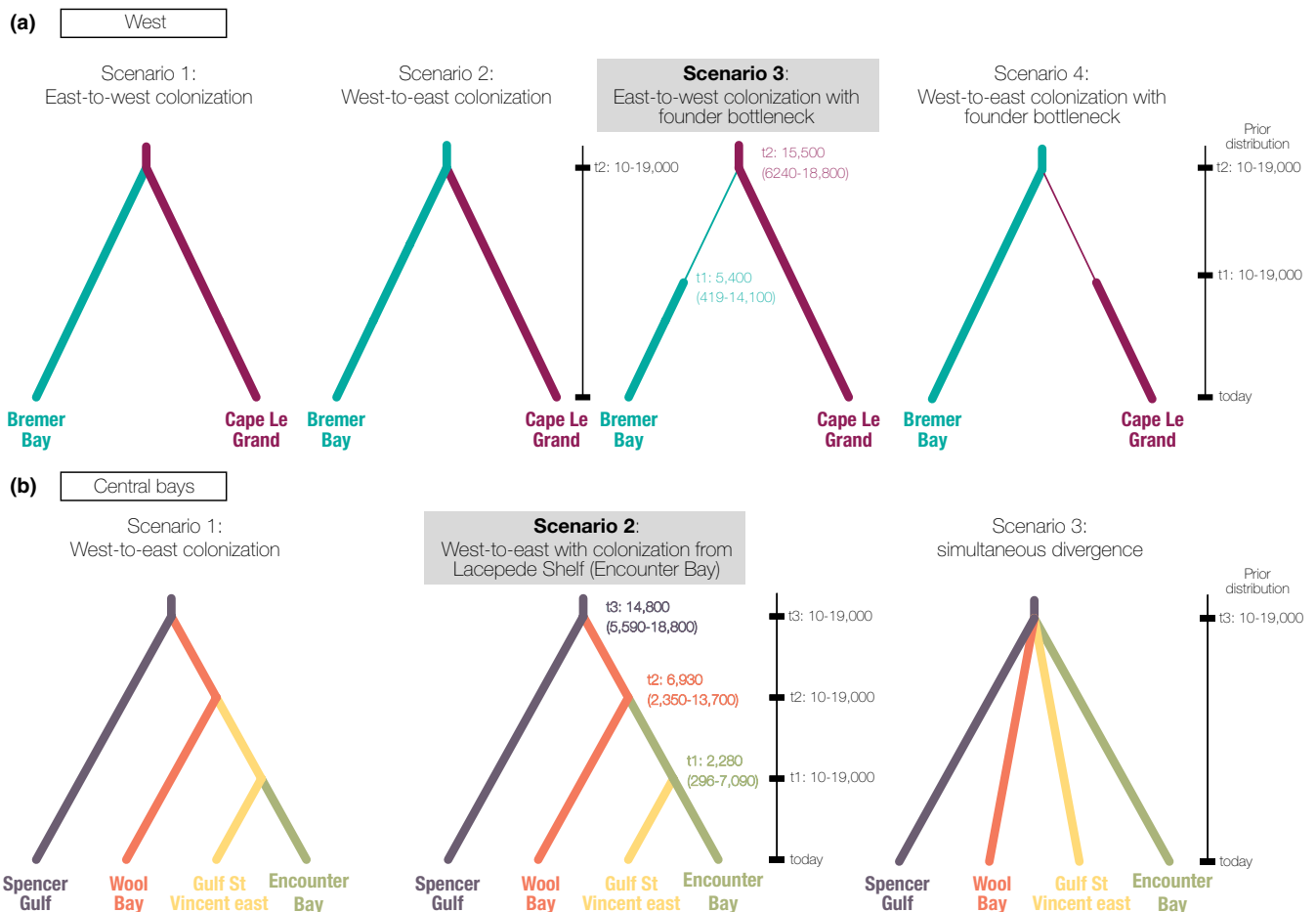
FIGURE 5 Scenarios tested in DIYABC for (a) the western group and (b) the central bays. The time scale on the right indicates priors for population events (Table S7). The chosen scenario is highlighted in bold and posterior estimates for population divergence times (median, 2.5% and 97.5% quartile) are annotated for this scenario. Colours correspond to population codes in Figure 1a

et al., 2012). In addition to this general gain in habitable area since the LGM, there were marked regional differences between the central and the western parts of the Great Southern Reef with respect to the amount of shallow seabed available during the LGM, the trajectory of increase, and the area available today (Figure 1c–e).

The amount of shallow seabed that was gained with sea-level rise since the LGM decreased from east to west across the seadragon's range (Figure 4). On the narrow western shelf, shallow seabed was particularly restricted during the LGM (229–1,154 km² over 2° of longitude) and modestly increased once sea level rose (Figure 1c). In the eastern part of the seadragon's range, more substantial shallow water areas remained during the LGM that could have served as refugia (2,251–3,682 km²). The trajectory of the marine transgression into the central bays was steep (Figure 1e) once the three bays started to flood about 12,000–11,000 years ago (Roberts et al., 2020), after which present-day sea level was reached quickly 8,000–7,500 years ago (Belperio et al., 2002). Today, there is over four times as much shallow seabed in the central bays compared to the western coast (81,250 vs. 19,626 km²). Depending on their location on the Great Southern Reef, populations experienced different magnitudes of environmental change when sea levels rose that may have manifested themselves in distinct population genetic responses.

4.2 | Contrasting patterns of genetic differentiation and diversity between the western and the central coast

We found opposite genetic patterns in leafy seadragon populations across their range that could be linked to the regional sea-level histories. Samples fell into two strongly differentiated clusters corresponding to the western and the central part of the coast, separated by the inaccessible and hence unsampled GAB (Figure 2). This broadest split of leafy seadragons has already been shown with microsatellites and mitochondrial DNA (Stiller et al., 2017) but adding individuals from Hopetoun and Lucky Bay narrowed the gap across the GAB from the west by ~250 km. Although genetic differentiation between the two clusters was large (minimum $F_{ST} = 0.491$, $F'_{ST} = 0.554$), small admixture proportions were shared between the closest localities across the GAB (Cape Le Grand in the west, Spencer Gulf in the east) indicating genetic connectivity. This conclusion is also supported by low divergence in mitochondrial DNA across the GAB (0.11%, Stiller et al., 2017). Our shelf reconstructions showed that the GAB maintained some of the largest shallow areas during the LGM (Figure 1d), which could have served as refugia for populations during sea-level lowstands.

The two main groups differed in genetic diversity, population structure and strength of expansion. Populations in the central bays sustained significantly higher genetic diversity than those in the western group (Figure 4; Table 2). This confirms the previously reported low heterozygosity in microsatellites among individuals sampled from Bremer Bay (Stiller et al., 2017) and suggests low genetic

diversity as a general pattern across the western part of the range. Both groups contained substructure but the degree of population differentiation was more gradual and less pronounced across wider geographical distances in the west than in the east (Figures 2 and 3a). In agreement with the expectation that coastal populations must have expanded following the LGM as in other parts of the world (Crandall et al., 2012; Jenkins et al., 2018), we detected signals of expansion in both the eastern and the western populations, but again with stronger signals in the east (Table 2). These patterns may be explained by different recolonization histories in relation to the postglacial flooding of the western and eastern areas.

4.3 | Spatial genetic structure in the western part of the Australian coast

Our extended sampling uncovered previously unknown genetic structure and a diversity cline in the western part of the leafy seadragon's range. The study by Stiller et al., (2017) was limited to a single population (Bremer Bay, $N = 10$), two individuals from Albany and four samples of unknown origin in Western Australia (Larson et al., 2014) and did not detect any substructure. Here, we found two main groups. In the far west, Peaceful Bay/Albany and Bremer Bay samples grouped together in DAPC and the lineage tree (Figure 2) and showed only weak allele frequency differences (Table 1). Further east, samples from Hopetoun and Cape Le Grand grouped together in DAPC and shared similar proportions of the two ancestry components in the region (Figure 2). A barrier between Hopetoun and Bremer Bay was also inferred by EEMS analysis showing a low effective migration rate (Figure 3b).

In contrast to the expectation that narrow shelves cause greater population genetic differentiation than wide shelves because habitat is less continuous (Dolby et al., 2018, 2020), we found shallower population structure on the narrow western margin than in the wide central bays. Notwithstanding the greater geographical distance spanned in the west (476 km least-cost distance), genetic differentiation did not reach the degree of differentiation between sites in the central bays that were just 251–298 km apart (Figure 3a). The shallow genetic structure among western sites was seen as dense clustering of samples in PCA, relatively uniform ancestry composition (Figure 2) and above average effective migration rates (Figure 3b). One explanation is that the western margin retained so little habitat during the LGM lowstand that populations were extirpated and subsequently recolonized from more eastern localities after sea level rose. Such a scenario was supported by a cline in genetic diversity and our phylogeographical modelling.

Genetic diversity (H_O) decreased in the western group from the easternmost locality (Cape Le Grand) towards the west (Peaceful Bay/Albany) and mirrored the amount of seabed gained since the LGM (Figure 4). This cline is consistent with a stepwise recolonization from a more eastern source in a series of founder events going westward (Excoffier et al., 2009; Slatkin & Excoffier, 2012). The topology of the SVDQUARTETS lineage tree also indicated a westward

splitting, with more eastern localities in the western group giving rise to individuals from further west (Figure 2e). Scenario testing, albeit only including two of four populations due to low sample sizes, also favoured the easternmost location Cape Le Grand giving rise to Bremer Bay, accompanied by a reduction of effective population size after colonization (Figure 5; Table S7). Interestingly, the inferred direction of the expansion is opposite to the flow of the Leeuwin Current, which indicates that dispersal with currents may not be the main factor structuring populations of leafy seadragons, in contrast to their kelp habitat (Coleman et al., 2011). Although the inferred age estimates have large uncertainties, the split of the western group was inferred to be relatively old (median 15,500 years; Table S7). This suggests that recolonization in the west may have begun shortly after sea levels started to rise after the LGM. The shallow population structure in the western regions suggests that narrow margins do not always display deep population structure (Dolby et al., 2020) if they were recolonized in a stepwise fashion by populations that persisted throughout the LGM on broader margins.

4.4 | Spatial genetic structure in the central part of the Australian coast

Substantial substructure was detected in the eastern part of the leafy seadragon's range. Genetically distinguishable groups were present in the western and the eastern Spencer Gulf, the western coast of Gulf St Vincent (Wool Bay), the eastern coast of Gulf St Vincent and Encounter Bay (Figure 2). This improves on an earlier analysis in which microsatellite allele frequency differences suggested substructure but STRUCTURE analyses failed to corroborate these observations (Stiller et al., 2017). The genetic structure in the bays of South Australia could reflect colonization of the large shallow areas following the LGM and subsequent reduction in gene flow among the bays. This scenario was supported by a pronounced expansion signal in all populations and differentiation between most populations (Tables 1 and 2). Once inside the bay after postglacial flooding, the distances to the next bay became longer, contributing to growing genetic differentiation of the weakly dispersive leafy seadragons. Life history is probably an important factor in maintaining the signal of postglacial isolation. This was also suggested for the California killifish, which attaches its eggs to vegetation, and showed greater differentiation compared to other estuarine fish species that were strongly admixed in postglacially formed habitats (Dolby et al., 2016, 2018). The proposed postglacial isolation in the central bays of Australia could be further studied with the remarkable diversity of 30 species of syngnathids in this area (Reef Watch, 2014), which are all brooders and presumably low dispersers and would thus be suitable models to extend studies of population structure in this complex part of the coast.

A puzzling finding was the relatively high differentiation across Gulf St Vincent. Populations on each side of the bay are just 69 km apart (least-cost path between 0 and 50 m depth), yet showed higher genetic differentiation than expected given the geographical proximity (Figure 3a) and were separated by a band of lower effective migration rates (Figure 3b). The two sides of Gulf St Vincent grouped more strongly with the next bay than with each other in PCA, in DAPC and in admixture components (Figure 2b–e) and mitochondrial haplotypes were shared between adjacent bays but not across Gulf St Vincent (Stiller et al., 2017). The differentiation across Gulf St Vincent may be explained by limited cross-bay dispersal. Connecting habitat may be missing from the deeper central areas of Gulf St Vincent (Edyvane, 2008). This differs from Spencer Gulf where vegetation is found in relatively central regions and where seadragons have been trawled from 15 to 26 m depth (Currie et al., 2009; Sorokin et al., 2009). If suitable habitat in Gulf St Vincent was indeed restricted to shallower coastal areas, the distance to cross the bay would increase to 220 km (least-cost path between 0 and 20 m depth; Figure S8). This distance makes the observed genetic differentiation between the sides of the gulf more consistent with the expectation of IBD (Figure 3a). Nonetheless, geography-agnostic approaches (PCA, DAPC, STRUCTURE) still supported stronger affinities of western Gulf St Vincent (Wool Bay) + Spencer Gulf and of eastern Gulf St Vincent + Encounter Bay, rather than an across-bay grouping. This suggests that genetic differentiation in the central bays is not solely explained by IBD.

Phylogeographical modeling supported that Gulf St Vincent was colonized twice, once from the west into Wool Bay around 6,930 years ago and a second time from the east (Encounter Bay) into eastern Gulf St Vincent around 2,280 years ago (Figure 5; Table S7). The exchange between Encounter Bay and Gulf St Vincent became possible after sea levels reached 30 m below today, ~10,000 years ago, when Kangaroo Island separated from the mainland (Roberts et al., 2020). Samples of leafy seadragons from Kangaroo Island would be particularly interesting to further investigate this second colonization of Gulf St Vincent. Our findings suggest that the differentiation across Gulf St Vincent stems from the colonization by two lineages and may have been maintained by the contemporary distribution of habitat in the Gulf.

Another possibility, yet speculative, is that western Gulf St Vincent received a recent pulse of gene flow with Spencer Gulf. When sea level was higher than today, an 8-km-wide marine strait formed across the southern portion of Yorke Peninsula at Peesey swamp (Figure 1a; Bourman et al., 2016; Pan et al., 2018). Deposits of marine life are present from the Last Interglacial Maximum, 128,000–116,000 years ago, when sea levels were 3–5 m higher than today (Pan et al., 2018). The strait may have also been open during the last highstand around 6,400 years ago (Bourman et al., 2016), when sea levels were 1–3 m above today (Belperio et al., 2002) but it is unknown if the passage supported suitable habitat to connect marine populations during this last opening. The possibility of a transient connectivity across Yorke Peninsula could be investigated by integrating more fine-scale reconstructions of historical coastal evolution and denser genetic sampling close to the former strait.

4.5 | Implications for global coastal phylogeography

In understanding which processes have shaped the biodiversity of the continental shelf, sea-level rise since the last glaciation is a prime factor because it has entirely overturned most shallow marine habitats. Our study suggests that contrasting population genetic responses may relate to the local topography of the shelf as it impacted the flooding trajectory after the LGM. The contrasting topologies of the continental shelf of the Great Southern Reef in Australia are not an isolated occurrence. In fact, several coastal systems have been identified where differences in habitable area throughout the glacial cycles were even stronger (Dolby et al., 2020; Holland, 2012). These could be studied in a framework integrating genetic assessment with historical coastline reconstructions as has been done in the northeast Pacific (Dolby et al., 2016, 2018) and here for southern Australia. In many regions, the impact of latitudinal temperature changes and glacial coverage of marine areas have to be taken into account as additional structuring factors (Hewitt, 2000; Jenkins et al., 2018; Maggs et al., 2008), which are less relevant along the east–west-facing Great Southern Reef with its large longitudinal extent and distance to glaciers. Suitable taxa to unveil patterns of sea-level impacts have limited dispersal, so that historical imprints are maintained for longer in the genome (Epps & Keyghobadi, 2015). Syngnathids are good models in this respect because they are brooders and often have reduced fins (Mobley et al., 2011; Wilson & Orr, 2011). Several seahorse and pipefish species show responses consistent with postglacial recolonization (Lourie et al., 2005; Wilson, 2006; Wilson & Eigenmann Veraguth, 2010), which could be further integrated with sea-level reconstructions to help understand the global significance of the interplay between shelf topography, sea-level rise and phylogeography of coastal populations.

AUTHOR CONTRIBUTIONS

J.S., N.G.W. and G.W.R. designed the research and performed sampling. J.S. performed laboratory work. R.R.F., M.E.A. and B.C.F. contributed new reagents and analytical tools. J.S. and R.R.F. analysed the data. J.S., N.G.W. and G.W.R. wrote the paper with input from all authors.

DATA AVAILABILITY STATEMENT

Raw sequence reads are archived in NCBI SRA under BioProject PRJNA624364. Code used in bioinformatic processing, bathymetry calculations, population genetic analyses and their output files is available on Zenodo:10.5281/zenodo.4268053.

ORCID

Josefin Stiller https://orcid.org/0000-0001-6009-9581
Rute R. da Fonseca https://orcid.org/0000-0002-2805-4698
Michael E. Alfaro https://orcid.org/0000-0002-8898-8230
Brant C. Faircloth https://orcid.org/0000-0002-1943-0217
Nerida G. Wilson https://orcid.org/0000-0002-0784-0200
Greg W. Rouse https://orcid.org/0000-0001-9036-9263

REFERENCES

Alfaro, M. E., Faircloth, B. C., Harrington, R. C., Sorenson, L., Friedman, M., Thacker, C. E., Oliveros, C. H., Černý, D., & Near, T. J. (2018). Explosive diversification of marine fishes at the cretaceous-palaeogene boundary. *Nature Ecology & Evolution*, *2*(4), 688–696. https://doi.org/10.1038/s41559-018-0494-6

Amante, C., & Eakins, B. W. (2009). ETOPO1 1 Arc-Minute Global Relief Model: Procedures, Data Sources and Analysis. *NOAA Technical Memorandum NESDIS NGDC-24*. National Geophysical Data Center, NOAA. https://doi.org/10.7289/V5C8276M. Accessed December 12, 2016.

Baker, J. L. (2002). *Dragon Search: Public report. Summary of Western Australian sighting data to September 2002. Report for Dragon Search community-based monitoring project*. Reef Watch.

Baker, J. L. (2005). *Dragon Search: Public report. Summary of Victorian sighting data to April 2005. Report for Dragon Search community-based monitoring project*. Reef Watch.

Baker, J. L. (2009). *Dragon Search: Public report. Summary of national sighting data, 1990 to 2005. Report for Dragon Search community-based monitoring program*. Reef Watch.

Belperio, A. P., Harvey, N., & Bourman, R. P. (2002). Spatial and temporal variability in the Holocene sea-level record of the South Australian coastline. *Sedimentary Geology*, *150*(1), 153–169. https://doi.org/10.1016/S0037-0738(01)00273-1

Bennett, S., Wernberg, T., Connell, S. D., Hobday, A. J., Johnson, C. R., & Poloczanska, E. S. (2016). The "Great Southern Reef": Social, ecological and economic value of Australia's neglected kelp forests. *Marine and Freshwater Research*, *67*(1), 47–56. https://doi.org/10.1071/MF15232

Besnier, F., & Glover, K. A. (2013). ParallelStructure: A R package to distribute parallel runs of the population genetics program STRUCTURE on multi-core computers. *PLoS One*, *8*(7), e70651. https://doi.org/10.1371/journal.pone.0070651

Bolger, A. M., Lohse, M., & Usadel, B. (2014). Trimmomatic: A flexible trimmer for Illumina sequence data. *Bioinformatics*, *30*(15), 2114–2120. https://doi.org/10.1093/bioinformatics/btu170

Bolton, J. J. (1994). Global seaweed diversity: Patterns and anomalies. *Botanica Marina*, *37*(3), 374. https://doi.org/10.1515/botm.1994.37.3.241

Bourman, R. P., Murray-Wallace, C. V., & Harvey, N. (2016). *Coastal landscapes of South Australia*. University of Adelaide Press.

Bowen, B. W., Gaither, M. R., DiBattista, J. D., Iacchei, M., Andrews, K. R., Grant, W. S., Toonen, R. J., & Briggs, J. C. (2016). Comparative phylogeography of the ocean planet. *Proceedings of the National Academy*

of Sciences of the United States of America, *113*(29), 7962–7969. https://doi.org/10.1073/pnas.1602404113

Braga Goncalves, I., Cornetti, L., Couperus, A. S., van Damme, C. J. G., & Mobley, K. B. (2017). Phylogeography of the snake pipefish, *Entelurus aequoreus* (family: Syngnathidae) in the northeastern Atlantic Ocean. *Biological Journal of the Linnean Society*, *122*(4), 787–800. https://doi.org/10.1093/biolinnean/blx112

Chifman, J., & Kubatko, L. (2014). Quartet inference from SNP data under the coalescent model. *Bioinformatics*, *30*(23), 3317–3324. https://doi.org/10.1093/bioinformatics/btu530

Coleman, M. A., Roughan, M., Macdonald, H. S., Connell, S. D., Gillanders, B. M., Kelaher, B. P., & Steinberg, P. D. (2011). Variation in the strength of continental boundary currents determines continent-wide connectivity in kelp. *The Journal of Ecology*, *99*(4), 1026–1032. https://doi.org/10.1111/j.1365-2745.2011.01822.x

Connolly, R. M., Melville, A. J., & Keesing, J. K. (2002). Abundance, movement and individual identification of leafy seadragons, *Phycodurus eques* (Pisces: Syngnathidae). *Marine and Freshwater Research*, *53*(4), 777–780. https://doi.org/10.1071/mf01168

Connolly, R. M., Melville, A. J., & Preston, K. M. (2002). Patterns of movement and habitat use by leafy seadragons tracked ultrasonically. *Journal of Fish Biology*, *61*(3), 684–695. https://doi.org/10.1111/j.1095-8649.2002.tb00904.x

Cornuet, J.-M., Pudlo, P., Veyssier, J., Dehne-Garcia, A., Gautier, M., Leblois, R., Marin, J.-M., & Estoup, A. (2014). DIYABC v2.0: A software to make approximate Bayesian computation inferences about population history using single nucleotide polymorphism, DNA sequence and microsatellite data. *Bioinformatics*, *30*(8), 1187–1189. https://doi.org/10.1093/bioinformatics/btt763

Cornuet, J.-M., Ravigné, V., & Estoup, A. (2010). Inference on population history and model checking using DNA sequence and microsatellite data with the software DIYABC (v1.0). *BMC Bioinformatics*, *11*, 401. https://doi.org/10.1186/1471-2105-11-401

Costello, M. J., & Chaudhary, C. (2017). Marine biodiversity, biogeography, deep-sea gradients, and conservation. *Current Biology*, *27*(13), 2051. https://doi.org/10.1016/j.cub.2017.06.015

Crandall, E. D., Sbrocco, E. J., Deboer, T. S., Barber, P. H., & Carpenter, K. E. (2012). Expansion dating: Calibrating molecular clocks in marine species from expansions onto the Sunda Shelf following the Last Glacial Maximum. *Molecular Biology and Evolution*, *29*(2), 707–719. https://doi.org/10.1093/molbev/msr227

Currie, D. R., Dixon, C. D., Roberts, S. D., Hooper, G., Sorokin, S., & Ward, T. (2009). *Fishery-independent by-catch survey to inform risk assessment of the Spencer Gulf prawn trawl fishery. Report to PIRSA Fisheries (SARDI Aquatic Sciences Publication No. F2009/000369-1)*. South Australian Research and Development Institute (Aquatic Sciences).

Curtis, J. M. R., & Vincent, A. C. J. (2006). Life history of an unusual marine fish: Survival, growth and movement patterns of *Hippocampus guttulatus* Cuvier 1829. *Journal of Fish Biology*, *68*(3), 707–733. https://doi.org/10.1111/j.0022-1112.2006.00952.x

Danecek P., Auton A., Abecasis G., Albers C. A., Banks E., DePristo M. A., Handsaker R. E., Lunter G., Marth G. T., Sherry S. T., McVean G., Durbin R., & 1000 Genomes Project Analysis Group (2011). The variant call format and VCFtools. *Bioinformatics*, *27*(15), 2156–2158. http://doi.org/10.1093/bioinformatics/btr330

DePristo, M. A., Banks, E., Poplin, R., Garimella, K. V., Maguire, J. R., Hartl, C., Philippakis, A. A., del Angel, G., Rivas, M. A., Hanna, M., McKenna, A., Fennell, T. J., Kernytsky, A. M., Sivachenko, A. Y., Cibulskis, K., Gabriel, S. B., Altshuler, D., & Daly, M. J. (2011). A framework for variation discovery and genotyping using next-generation DNA sequencing data. *Nature Genetics*, *43*(5), 491–498. https://doi.org/10.1038/ng.806

Dolby, G. A., Bedolla, A. M., Bennett, S. E. K., & Jacobs, D. K. (2020). Global physical controls on estuarine habitat distribution during sea level change: Consequences for genetic diversification through time. *Global and Planetary Change*, *187*, 103128. https://doi.org/10.1016/j.gloplacha.2020.103128

Dolby, G. A., Ellingson, R. A., Findley, L. T., & Jacobs, D. K. (2018). How sea level change mediates genetic divergence in coastal species across regions with varying tectonic and sediment processes. *Molecular Ecology*, *27*(4), 994–1011. https://doi.org/10.1111/mec.14487

Dolby, G. A., Hechinger, R., Ellingson, R. A., Findley, L. T., Lorda, J., & Jacobs, D. K. (2016). Sea-level driven glacial-age refugia and post-glacial mixing on subtropical coasts, a palaeohabitat and genetic study. *Proceedings of the Royal Society B: Biological Sciences*, *283*(1843), 20161571. https://doi.org/10.1098/rspb.2016.1571

Dray, S., Dufour, A.-B., & Others. (2007). The ade4 package: Implementing the duality diagram for ecologists. *Journal of Statistical Software*, *22*(4), 1–20. https://doi.org/10.18637/jss.v022.i04

Earl, D. A., & vonHoldt, B. M. (2012). Structure harvester: A website and program for visualizing STRUCTURE output and implementing the Evanno method. *Conservation Genetics Resources*, *4*(2), 359–361. https://doi.org/10.1007/s12686-011-9548-7

Edyvane, K. S. (2008). Macroalgal biogeography and assemblages of Gulf St Vincent. In S. Shepherd, S. Bryars, I. R. Kirkegaard, P. Harbison, & J. Jennings (Eds.), *The natural history of Gulf St Vincent* (pp. 248–263). Royal Society of South Australia.

Epps, C. W., & Keyghobadi, N. (2015). Landscape genetics in a changing world: Disentangling historical and contemporary influences and inferring change. *Molecular Ecology*, *24*(24), 6021–6040. https://doi.org/10.1111/mec.13454

Eren, A. M., Esen, Ö. C., Quince, C., Vineis, J. H., Morrison, H. G., Sogin, M. L., & Delmont, T. O. (2015). Anvi'o: An advanced analysis and visualization platform for 'omics data. *PeerJ*, *3*, e1319. https://doi.org/10.7717/peerj.1319

Etherington, T. R. (2016). Least-cost modelling and landscape ecology: Concepts, applications, and opportunities. *Current Landscape Ecology Reports*, *1*(1), 40–53. https://doi.org/10.1007/s40823-016-0006-9

Evanno, G., Regnaut, S., & Goudet, J. (2005). Detecting the number of clusters of individuals using the software structure: A simulation study. *Molecular Ecology*, *14*(8), 2611–2620. https://doi.org/10.1111/j.1365-294X.2005.02553.x

Excoffier, L., Foll, M., & Petit, R. J. (2009). Genetic consequences of range expansions. *Annual Review of Ecology, Evolution, and Systematics*, *40*, 481–501. https://doi.org/10.1146/annurev.ecolsys.39.110707.173414

Faircloth, B. C. (2013). *Illumiprocessor: A trimmomatic wrapper for parallel adapter and quality trimming*. https://doi.org/10.6079/J9ILL

Faircloth, B. C. (2016). PHYLUCE is a software package for the analysis of conserved genomic loci. *Bioinformatics*, *32*(5), 786–788. https://doi.org/10.1093/bioinformatics/btv646

Faircloth, B. C., & Glenn, T. C. (2012). Not all sequence tags are created equal: Designing and validating sequence identification tags robust to indels. *PLoS One*, *7*(8), e42543. https://doi.org/10.1371/journal.pone.0042543

Faircloth, B. C., McCormack, J. E., Crawford, N. G., Harvey, M. G., Brumfield, R. T., & Glenn, T. C. (2012). Ultraconserved elements anchor thousands of genetic markers spanning multiple evolutionary timescales. *Systematic Biology*, *61*(5), 717–726. https://doi.org/10.1093/sysbio/sys004

Faircloth, B. C., Sorenson, L., Santini, F., & Alfaro, M. E. (2013). A phylogenomic perspective on the radiation of ray-finned fishes based upon targeted sequencing of ultraconserved elements (UCEs). *PLoS One*, *8*(6), e65923. https://doi.org/10.1371/journal.pone.0065923

Glenn, T. C., Nilsen, R. A., Kieran, T. J., Sanders, J. G., Bayona-Vásquez, N. J., Finger, J. W., Pierson, T. W., Bentley, K. E., Hoffberg, S. L., Louha, S., Garcia-De Leon, F. J., Del Rio Portilla, M. A., Reed, K. D., Anderson, J. L., Meece, J. K., Aggrey, S. E., Rekaya, R., Alabady, M., Belanger, M., … Faircloth, B. C. (2019). Adapterama I: Universal stubs

and primers for 384 unique dual-indexed or 147,456 combinatorial-ly-indexed Illumina libraries (iTru & iNext). *PeerJ*, *7*, e7755. https://doi.org/10.7717/peerj.7755

Goudet, J. (1995). FSTAT (version 1.2): A computer program to calculate F-statistics. *The Journal of Heredity*, *86*(6), 485–486. https://doi.org/10.1093/oxfordjournals.jhered.a111627

Hanebuth, T. J. J., Stattegger, K., & Grootes, P. M. (2000). Rapid flooding of the Sunda shelf: A late-glacial sea-level record. *Science*, *288*(5468), 1033–1035. https://doi.org/10.1126/science.288.5468.1033

Harris, P. T., Macmillan-Lawler, M., Rupp, J., & Baker, E. K. (2014). Geomorphology of the oceans. *Marine Geology*, *352*, 4–24. https://doi.org/10.1016/j.margeo.2014.01.011

Heap, A. D., & Harris, P. T. (2008). Geomorphology of the Australian margin and adjacent seafloor. *Australian Journal of Earth Sciences*, *55*(4), 555–585. https://doi.org/10.1080/08120090801888669

Hedrick, P. W. (2005). A standardized genetic differentiation measure. *Evolution*, *59*(8), 1633–1638. https://doi.org/10.1111/j.0014-3820.2005.tb01814.x

Hewitt, G. (2000). The genetic legacy of the quaternary ice ages. *Nature*, *405*(6789), 907–913. https://doi.org/10.1038/35016000

Holland, S. M. (2012). Sea level change and the area of shallow-marine habitat: Implications for marine biodiversity. *Paleobiology*, *38*(2), 205–217. https://doi.org/10.1666/11030.1

Jenkins, T. L., Castilho, R., & Stevens, J. R. (2018). Meta-analysis of northeast Atlantic marine taxa shows contrasting phylogeographic patterns following post-LGM expansions. *PeerJ*, *6*, e5684. https://doi.org/10.7717/peerj.5684

Jombart, T. (2008). adegenet: A R package for the multivariate analysis of genetic markers. *Bioinformatics*, *24*(11), 1403–1405. https://doi.org/10.1093/bioinformatics/btn129

Jombart, T., Devillard, S., & Balloux, F. (2010). Discriminant analysis of principal components: A new method for the analysis of genetically structured populations. *BMC Genetics*, *11*, 94. https://doi.org/10.1186/1471-2156-11-94

Kerswell, A. P. (2006). Global biodiversity patterns of benthic marine algae. *Ecology*, *87*(10), 2479–2488.

Kopelman, N. M., Mayzel, J., Jakobsson, M., Rosenberg, N. A., & Mayrose, I. (2015). Clumpak: a program for identifying clustering modes and packaging population structure inferences across K. *Molecular Ecology Resources*, *15*(5), 1179–1191. https://doi.org/10.1111/1755-0998.12387

Kuiter, R. H. (2000). *Seahorses, pipefishes and their relatives: A comprehensive guide to Syngnathiformes*. TMC Publishing.

Lambeck, K., & Chappell, J. (2001). Sea level change through the last glacial cycle. *Science*, *292*(5517), 679–686. https://doi.org/10.1126/science.1059549

Larson, S., Ramsey, C., Tinnemore, D., & Amemiya, C. (2014). Novel microsatellite loci variation and population genetics within leafy seadragons, *Phycodurus eques*. *Diversity*, *6*(1), 33–42. https://doi.org/10.3390/d6010033

Lewis, S. E., Sloss, C. R., Murray-Wallace, C. V., Woodroffe, C. D., & Smithers, S. G. (2013). Post-glacial sea-level changes around the Australian margin: A review. *Quaternary Science Reviews*, *74*, 115–138. https://doi.org/10.1016/j.quascirev.2012.09.006

Li, H. (2011). A statistical framework for SNP calling, mutation discovery, association mapping and population genetical parameter estimation from sequencing data. *Bioinformatics*, *27*(21), 2987–2993. https://doi.org/10.1093/bioinformatics/btr509

Li, H., & Durbin, R. (2009). Fast and accurate short read alignment with Burrows-Wheeler transform. *Bioinformatics*, *25*(14), 1754–1760. https://doi.org/10.1093/bioinformatics/btp324

Li, H., Handsaker, B., Wysoker, A., Fennell, T., Ruan, J., Homer, N., Marth, G., Abecasis, G., Durbin, R., & 1000 Genome Project Data Processing Subgroup (2009). The sequence alignment/map format and SAMtools. *Bioinformatics*, *25*(16), 2078–2079. https://doi.org/10.1093/bioinformatics/btp352

Lourie, S. A., Green, D. M., & Vincent, A. C. J. (2005). Dispersal, habitat differences, and comparative phylogeography of Southeast Asian seahorses (Syngnathidae: *Hippocampus*). *Molecular Ecology*, *14*(4), 1073–1094. https://doi.org/10.1111/j.1365-294X.2005.02464.x

Ludt, W. B., & Rocha, L. A. (2015). Shifting seas: The impacts of Pleistocene sea-level fluctuations on the evolution of tropical marine taxa. *Journal of Biogeography*, *42*(1), 25–38. https://doi.org/10.1111/jbi.12416

Maggs, C. A., Castilho, R., Foltz, D., Henzler, C., Jolly, M. T., Kelly, J., Olsen, J., Perez, K. E., Stam, W., Väinölä, R., Viard, F., & Wares, J. (2008). Evaluating signatures of glacial refugia for North Atlantic benthic marine taxa. *Ecology*, *89*(11 Suppl), S108–S122. https://doi.org/10.1890/08-0257.1

McCormack, J. E., Faircloth, B. C., Crawford, N. G., Gowaty, P. A., Brumfield, R. T., & Glenn, T. C. (2012). Ultraconserved elements are novel phylogenomic markers that resolve placental mammal phylogeny when combined with species-tree analysis. *Genome Research*, *22*(4), 746–754. https://doi.org/10.1101/gr.125864.111

McKenna, A., Hanna, M., Banks, E., Sivachenko, A., Cibulskis, K., Kernytsky, A., Garimella, K., Altshuler, D., Gabriel, S., Daly, M., & DePristo, M. A. (2010). The genome analysis toolkit: A MapReduce framework for analyzing next-generation DNA sequencing data. *Genome Research*, *20*(9), 1297–1303. https://doi.org/10.1101/gr.107524.110

Meirmans, P. G. (2012). The trouble with isolation by distance. *Molecular Ecology*, *21*(12), 2839–2846. https://doi.org/10.1111/j.1365-294X.2012.05578.x

Meirmans, P. G. (2020). Genodive version 3.0: Easy-to-use software for the analysis of genetic data of diploids and polyploids. *Molecular Ecology Resources*, *152*, 763. https://doi.org/10.1111/1755-0998.13145

Miller, M. A., Pfeiffer, W., & Schwartz, T. (2010). *Creating the CIPRES Science Gateway for inference of large phylogenetic trees*. Gateway Computing Environments Workshop (GCE).

Mobley, K. B., Small, C. M., & Jones, A. G. (2011). The genetics and genomics of Syngnathidae: Pipefishes, seahorses and seadragons. *Journal of Fish Biology*, *78*(6), 1624–1646. https://doi.org/10.1111/j.1095-8649.2011.02967.x

Murray-Wallace, C. V. (2014). The continental shelves of SE Australia. In F. L. Chiocci, & A. R. Chivas (Eds.), *Continental shelves of the world: Their evolution during the last glacio-eustatic cycle* (pp. 273–291). Geological Society, London, Memoirs.

Pan, T.-Y., Murray-Wallace, C. V., Dosseto, A., & Bourman, R. P. (2018). The last interglacial (MIS 5e) sea level highstand from a tectonically stable far-field setting, Yorke Peninsula, southern Australia. *Marine Geology*, *398*, 126–136. https://doi.org/10.1016/j.margeo.2018.01.012

Pante, E., & Simon-Bouhet, B. (2013). marmap: A package for importing, plotting and analyzing bathymetric and topographic data in R. *PLoS One*, *8*(9), e73051. https://doi.org/10.1371/journal.pone.0073051

Paradis, E. (2010). pegas: An R package for population genetics with an integrated–modular approach. *Bioinformatics*, *26*(3), 419–420. https://doi.org/10.1093/bioinformatics/btp696

Peter, B. M., Petkova, D., & Novembre, J. (2019). Genetic landscapes reveal how human genetic diversity aligns with geography. *Molecular Biology and Evolution*, *37*(4), 943–951. https://doi.org/10.1093/molbev/msz280

Petkova, D., Novembre, J., & Stephens, M. (2016). Visualizing spatial population structure with estimated effective migration surfaces. *Nature Genetics*, *48*(1), 94–100. https://doi.org/10.1038/ng.3464

Pritchard, J. K., Stephens, M., & Donnelly, P. (2000). Inference of population structure using multilocus genotype data. *Genetics*, *155*(2), 945–959.

Provan, J., & Bennett, K. D. (2008). Phylogeographic insights into cryptic glacial refugia. *Trends in Ecology & Evolution*, *23*(10), 564–571. https://doi.org/10.1016/j.tree.2008.06.010

Roberts, A. L., Mollenmans, A., Rigney, L.-I., & Bailey, G. (2020). Marine transgression, Aboriginal narratives and the creation of Yorke Peninsula/Guuranda, South Australia. *The Journal of Island and Coastal Archaeology*, *15*(3), 305–332. https://doi.org/10.1080/15564894.2019.1570990

Rohland, N., & Reich, D. (2012). Cost-effective, high-throughput DNA sequencing libraries for multiplexed target capture. *Genome Research*, *22*(5), 939–946. https://doi.org/10.1101/gr.128124.111

Sanchez-Camara, J., Booth, D. J., & Turon, X. (2005). Reproductive cycle and growth of *Phyllopteryx taeniolatus*. *Journal of Fish Biology*, *67*(1), 133–148. https://doi.org/10.1111/j.0022-1112.2005.00720.x

Shepherd, S., & Edgar, G. (2013). *Ecology of Australian temperate reefs: The unique south*. CSIRO Publishing.

Slatkin, M., & Excoffier, L. (2012). Serial founder effects during range expansion: A spatial analog of genetic drift. *Genetics*, *191*(1), 171–181. https://doi.org/10.1534/genetics.112.139022

Smith, B. T., Harvey, M. G., Faircloth, B. C., Glenn, T. C., & Brumfield, R. T. (2014). Target capture and massively parallel sequencing of ultraconserved elements for comparative studies at shallow evolutionary time scales. *Systematic Biology*, *63*(1), 83–95. https://doi.org/10.1093/sysbio/syt061

Sorokin, S. J., Connolly, R. M., & Currie, D. R. (2009). *Syngnathids of the Spencer Gulf: Morphometrics and isotopic signatures. Report to Nature Foundation SA Inc (SARDI Publication No. F2009/000655-1)*. South Australian Research and Development Institute (Aquatic Sciences).

Stiller, J., Wilson, N. G., Donnellan, S., & Rouse, G. W. (2017). The leafy seadragon, *Phycodurus eques*, a flagship species with low but structured genetic variability. *The Journal of Heredity*, *108*(2), 152–162. https://doi.org/10.1093/jhered/esw075

Swafford, D. L. (2002). *PAUP*. Phylogenetic analysis using parsimony (* and other models). Version 4.0 b10 for Macintosh*. Sinauer Associates Inc.

Reef Watch. (2014). *Seadragons and their Friends. A guide to Syngnathidae fishes in South Australia*. Conservation Council of South Australia.

White, N. D., & Braun, M. J. (2019). Extracting phylogenetic signal from phylogenomic data: Higher-level relationships of the nightbirds (Strisores). *Molecular Phylogenetics and Evolution*, *141*, 106611. https://doi.org/10.1016/j.ympev.2019.106611

Williams, A. N., Ulm, S., Sapienza, T., Lewis, S., & Turney, C. S. M. (2018). Sea-level change and demography during the last glacial termination and early Holocene across the Australian continent. *Quaternary Science Reviews*, *182*, 144–154. https://doi.org/10.1016/j.quascirev.2017.11.030

Wilson, A. B. (2006). Genetic signature of recent glaciation on populations of a near-shore marine fish species (*Syngnathus leptorhynchus*). *Molecular Ecology*, *15*(7), 1857–1871. https://doi.org/10.1111/j.1365-294X.2006.02911.x

Wilson, A. B., & Eigenmann Veraguth, I. (2010). The impact of Pleistocene glaciation across the range of a widespread European coastal species. *Molecular Ecology*, *19*(20), 4535–4553. https://doi.org/10.1111/j.1365-294X.2010.04811.x

Wilson, A. B., & Orr, J. W. (2011). The evolutionary origins of Syngnathidae: Pipefishes and seahorses. *Journal of Fish Biology*, *78*(6), 1603–1623. https://doi.org/10.1111/j.1095-8649.2011.02988.x

Yokoyama, Y., Lambeck, K., De Deckker, P., Johnston, P., & Keith Fifield, L. (2000). Timing of the last glacial maximum from observed sea-level minima. *Nature*, *406*(6797), 713–716. https://doi.org/10.1038/35021035

Zerbino, D. R., & Birney, E. (2008). Velvet: Algorithms for de novo short read assembly using de Bruijn graphs. *Genome Research*, *18*(5), 821–829. https://doi.org/10.1101/gr.074492.107

SUPPORTING INFORMATION

Additional supporting information may be found online in the Supporting Information section.